Thermal conductivity of Si/SiGe superlattice nanowires

Deyu Li
Department of Mechanical Engineering, University of California, Berkeley, California 94720

Yiying Wu, Rong Fan, and Peidong Yang[a)]
Department of Chemistry, University of California, Berkeley, California 94720

Arun Majumdar[a),b)]
Department of Mechanical Engineering, University of California, Berkeley, California 94720

(Received 16 June 2003; accepted 20 August 2003)

The thermal conductivities of individual single crystalline Si/SiGe superlattice nanowires with diameters of 58 and 83 nm were measured over a temperature range from 20 to 320 K. The observed thermal conductivity shows similar temperature dependence as that of two-dimensional Si/SiGe superlattice films. Comparison with the thermal conductivity data of intrinsic Si nanowires suggests that alloy scattering of phonons in the Si–Ge segments is the dominant scattering mechanism in these superlattice nanowires. In addition, boundary scattering also contributes to thermal conductivity reduction. © *2003 American Institute of Physics.* [DOI: 10.1063/1.1619221]

Semiconductor superlattices are attracting increasing attention due to their potential applications in thermoelectric and optoelectronic devices.[1,2] Control of thermal conductivity of semiconductor superlattice films is important because lower thermal conductivity could greatly improve the material's thermoelectric figure-of-merit in cooling and power generation applications and pose challenging thermal management problems for optoelectronic applications. While two-dimensional (2D) superlattice structures show promising properties,[3–9] one-dimensional superlattice nanowires may possess even more desirable characteristics and further improve device performance.[10] Recently, block-by-block growth of single crystalline Si/SiGe superlattice nanowires was achieved.[11] In this letter, we report the results of thermal conductivity measurements on individual Si/SiGe superlattice nanowires. The observed thermal conductivity indicates that alloy scattering in the SiGe segments is the dominant phonon scattering mechanism, while additional scattering mechanisms such as nanowire boundary scattering also contribute to thermal conductivity reduction.

The superlattice nanowires were synthesized by a hybrid pulsed laser ablation/chemical vapor deposition process[11] based on vapor-liquid-solid mechanism.[12,13] A (111) Si wafer coated with 5 nm Au thin film was inserted in a quartz furnace tube at 910 °C. A gas mixture of 10% $SiCl_4$ + 9% H_2 + 81% Ar was continuously introduced into the reaction tube with a flow rate of 400 sccm. At high temperatures, the Au thin film forms a liquid alloy with Si and spontaneously breaks up into nanometer-sized droplets. Si nanowires grow by precipitation at the liquid-solid interface. To form the SiGe sections, Ge vapor was generated periodically through the pulsed laser ablation of a pure Ge target with a frequency doubled Nd:yttritium–aluminum–garnet laser. The laser was programmed to turn on and off every 10 s. The typical average Ge concentration in the SiGe sections was between 5% and 10%. Selected-area-electron-diffraction pattern and high-resolution transmission electron microscopy (TEM)[11] show that the nanowires were nearly dislocation-free single crystalline and grew along the ⟨111⟩ direction with a superlattice period ranging from 50 to 150 nm depending on the diameter. Figure 1(a) shows a TEM image of a Si/SiGe nanowire. The interface between Si and SiGe can be readily seen in Fig. 1(a). However, it is not expected to be as sharp as epitaxial superlattice films due to diffusion at high synthesis temperature.

The thermal conductivity measurement was performed with a microdevice[14–16] consisting of two silicon nitride (SiN_x) membranes, each suspended by five SiN_x beams that

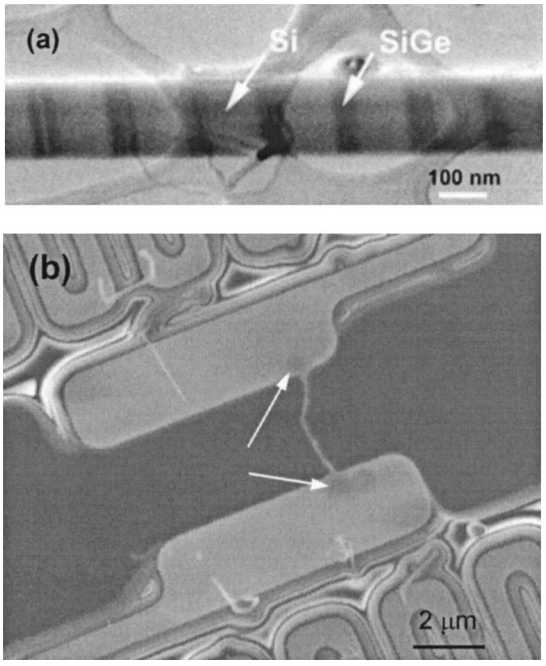

FIG. 1. (a) A transmission electron micrograph of a Si/SiGe superlattice nanowire. (b) A scanning electron micrograph of an 83 nm Si/SiGe superlattice nanowire bridging the two suspended heater pads. The arrows point to the carbon deposits.

[a)]Also at: Materials Science Division, Lawrence Berkeley National Laboratory, Berkeley, California, 94720.
[b)]Electronic mail: majumdar@me.berkeley.edu

were 420 μm long. A thin Pt resistance coil (used as both heater and resistance thermometer) and a separate Pt electrode were patterned on each membrane and electrically connected to contact pads by metal lines on the suspended legs. Solution drop-dry method[14] were used to place a nanowire in-between the two suspended membranes and amorphous carbon films were locally deposited at the nanowire-heater pad junctions with a scanning electron microscope (SEM). Estimation similar to that in Ref. 15 shows that the error introduced from the contact should be less than 4% for the Si/SiGe superlattice nanowires after this contact treatment. A SEM image of an 83 nm diameter Si/SiGe superlattice nanowire bridging the two suspended pads is shown in Fig. 1(b).

All measurements were performed in a cryostat at a vacuum level $\sim 2\times 10^{-6}$ Torr. To a very accurate approximation, the nanowire forms the only heat path between the two suspended heater islands. A bias voltage applied to the heating resistor, R_h, creates joule heating and increases the temperature, T_h, of the heater island above the thermal bath temperature, T_0. Under steady state, part of the heat transfers through the nanowire to the sensing resistor, R_s, and raises its temperature, T_s. Solving the heat transfer equations of the system,[15] denoting the thermal conductance of the wire, G_w, and the suspending legs, G_l, we have, $T_h = T_0 + [(G_l + G_w)/G_l(G_l + 2G_w)]P$, and $T_s = T_0 + [G_w/G_l(G_l + 2G_w)]P$, where $P = I^2(R_h + R_l/2)$. Here R_l is the total electrical lead resistance of Pt lines that connects the heater coil. The nanowire thermal conductance and, hence, the thermal conductivity can be then derived. During the experiments, the maximum power dissipation at the heating side was below 1 μW and the maximum temperature rise at the heating side was below 5 K.

Thermal conductivities of 58 and 83 nm diameter single crystalline Si/SiGe superlattice nanowires were measured from 20 to 320 K, as shown in Fig. 2(a). For comparison, the thermal conductivities of a 2D $Si/Si_{0.7}Ge_{0.3}$ superlattice film (3 μm thick with 30 nm period) and a $Si_{0.9}Ge_{0.1}$ alloy film (3.5 μm thick) are also shown.[6,7] In addition, Fig. 2(b) shows the thermal conductivities of intrinsic single crystalline Si nanowires of different diameters.[16] The thermal conductivity of the Si/SiGe nanowire increases rapidly from 20 to 200 K, and then increases only marginally for $T > 200$ K, which is quite similar to the behavior of the 2D superlattice film. However, the value of the nanowire thermal conductivity is only about half of that of the 2D $Si/Si_{0.7}Ge_{0.3}$ superlattice film.

Heat transport in the superlattices can be controlled by several phonon scattering mechanisms,[17,18] namely: (i) alloy scattering; (ii) interface scattering due to mismatch in acoustic impedance; and (iii) scattering by defects and dislocations at interfaces created due to lattice mismatch. It is worth noting that for Si_xGe_{1-x}, both the lattice parameter and the acoustic impedance can be estimated as a linear combination of the respective Si and Ge properties. Systematic studies[4–7] on $Si_xGe_{1-x}/Si_yGe_{1-y}$ 2D superlattices have suggested the following scenario. When $|x-y| \leqslant 0.1$, acoustic impedance and lattice mismatches in the two materials are sufficiently small that interfacial phonon scattering is marginal whereas alloy scattering is dominant, rendering the superlattice structure unimportant. When $|x-y| \approx 0.3$, the lattice mismatch is still sufficiently low that, depending on the growth conditions, the generation of interfacial defects and dislocations can be reduced or eliminated.[6,7] However, the acoustic impedance mismatch is large enough for phonon reflection at the interfaces to be the dominant scattering mechanism. In such cases, although the superlattice thermal conductivity is inversely proportional to the interfacial density, it is difficult to decrease the thermal conductivity below the alloy scattering limit, i.e., if the $Si_xGe_{1-x}/Si_yGe_{1-y}$ superlattice is mixed homogenously into an alloy. For $|x-y| \geqslant 0.6$, however, the lattice mismatch is large enough for crystal imperfections to be generated at the interface (i.e., if the period is thicker than the critical thickness determined by the strain created by lattice mismatch),[19] which dominate phonon scattering. In such cases, the superlattice thermal conductivity is generally lower than the alloy scattering limit and depends on the defect and dislocation density, and their structure, which are difficult to predict. In the case of our nanowire samples, since $|x-y| < 0.1$, generation of misfit dislocations and defects is unlikely, as evidenced in our TEM studies. The lengths of the nanowires between the two heater pads are 2.08 and 2.86 μm for the 58 and the 83 nm diameter nanowires, respectively. The period of the nanowires depends on the wire diameter and increases roughly linearly with the wire diameter.[11] However, since the diameters of these two wires are not very different, their periods are not very different either, and lie between 100 and 150 nm. Within the mea-

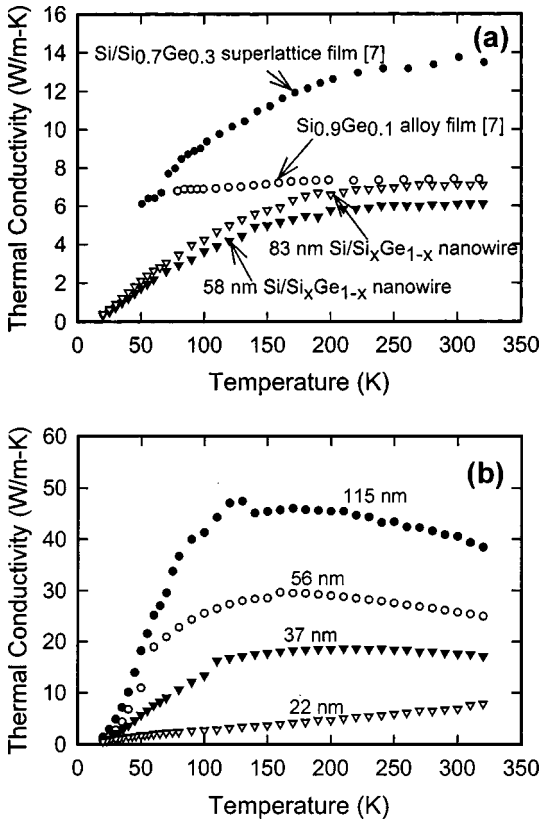

FIG. 2. (a) Thermal conductivities of 58 and 83 nm diameter single crystalline Si/Si_xGe_{1-x} superlattice nanowires. The value of x is $\sim 0.9-0.95$ and the superlattice period is 100–150 nm. Thermal conductivities of a 30 nm period 2D $Si/Si_{0.7}Ge_{0.3}$ superlattice film and $Si_{0.9}Ge_{0.1}$ alloy film (3.5 μm thick) are also shown. (b) Thermal conductivities of single crystalline pure Si nanowires. The number besides each curve denotes the corresponding wire diameter.

surement section, there are only a small number of interfaces (<28 interfaces) present. This leads us to believe that interface scattering is not very significant because both the acoustic impedance mismatch and the number of interfaces are small. Based on 2D superlattice studies, one expects alloy scattering to dominate the thermal conductivity of our nanowires. While we believe this is indeed the case for the nanowires, it is important to point out that the thermal conductivity of superlattice nanowires, for which $|x-y|<0.1$ and period $\approx 100-150$ nm, was found to be lower by a factor of 2 compared with that of 2D superlattice film for which $|x-y|=0.3$ and period ≈ 30 nm. This leads us to believe that in addition to alloy scattering, nanowire boundary scattering should also be taken into account.

Comparison with the results in Fig. 2(b) shows that the thermal conductivities of the Si/SiGe superlattice nanowires are much lower than those of pure Si ones of similar diameters. This also suggests that the predominant scattering mechanism is alloy scattering in the SiGe regions. However, the fact that the thermal conductivity of the 58 nm diameter wire is smaller than that of the 83 nm diameter wire indicates that the phonon scattering by the nanowire boundary is also important. Note that because of the strong alloy scattering, the boundary scattering effect for superlattice wires is not as significant as that for Si wires, whose thermal conductivity shows a much pronounced diameter dependence. This is also the reason for that the thermal conductivity of superlattice nanowires never decreases with increasing temperature between 20 and 320 K. This is because alloy scattering dominates over phonon–phonon Umklapp scattering.

How could both scattering mechanisms play a role? According to Rayleigh scattering theory, the phonon scattering efficiency of atomic scale defects follows the fourth power of the ratio of the defect size to phonon wavelength. Since alloys are composed of atomic scale lattice imperfections, they can efficiently scatter short-wavelength (high-frequency) acoustic phonons, while scattering of long-wavelength phonons remains ineffective. We believe that in addition to alloy scattering of short-wavelength phonons in the superlattice nanowires, the nanowire boundary provides an effective scattering mechanism for the long-wavelength phonons. This additional phonon scattering mechanism further reduces the thermal conductivity below that of 2D superlattices. Since the role of long-wavelength acoustic phonons in thermal transport becomes more dominant at lower temperatures, one would expect the discrepancy between the thermal conductivity of bulk alloy and our superlattice nanowires to be higher at lower temperatures. This is indeed observed in Fig. 2(a).

In summary, the thermal conductivities of 58 and 83 nm diameter Si/SiGe single crystalline superlattice nanowires were measured. Comparison with the results of pure Si nanowires suggests that alloy scattering is the dominant phonon scattering mechanism for the thermal transport in these wires. However, nanowire boundary scattering is also important in reducing the thermal conductivity. A possible explanation is that while short-wavelength acoustic phonons are effectively scattered by atomic scale point imperfections in the SiGe alloy segments, long-wavelength acoustic phonons are scattered by the nanowire boundary.

The authors wish to thank Dr. P. Kim, Dr. L. Shi, and Dr. S. Huxtable for helpful discussions and acknowledge the support of the NSF NIRT project and the DOE NSE project.

[1] X. Fan, G. Zeng, C. LaBounty, J. Bowers, E. Croke, C. Ahn, S. Huxtable, A. Majumdar, and A. Shakouri, Appl. Phys. Lett. **78**, 1580 (2001).
[2] M. R. Kitchin, M. J. Shaw, E. Corbin, J. P. Hagon, and M. Jaros, Phys. Rev. B **61**, 8375 (2000).
[3] R. Venkatasubramanian, E. Silvola, T. Colpitts, and B. O'Quinn, Nature (London) **413**, 597 (2001).
[4] S.-M. Lee, D. G. Cahill, and R. Venkatasubramanian, Appl. Phys. Lett. **70**, 2957 (1997).
[5] T. Borca-Tasciuc, W. Liu, J. Liu, T. Zeng, D. Song, C. Moore, G. Chen, K. Wang, T. Radetic, R. Gronsky, T. Koga, and M. S. Dresselhaus, Superlattices Microstruct. **28**, 199 (2000).
[6] S. T. Huxtable, A. R. Abramson, C.-L. Tien, A. Majumdar, C. Labounty, X. Fan, G. Zeng, J. Bowers, A. Shakouri, and E. Croke, Appl. Phys. Lett. **80**, 1737 (2002).
[7] S. Huxtable, Ph.D thesis, University of California, Berkeley, 2002; http://nano.me.berkeley.edu
[8] M. N. Touzelbaev, P. Zhou, R. Venkatasubramanian, and K. E. Goodson, J. Appl. Phys. **90**, 763 (2001).
[9] W. Capinski and H. J. Maris, Physica B **219&220**, 699 (1996).
[10] M. S. Dresselhaus, Y. M. Lin, S. B. Cronin, O. Rabin, M. R. Black, G. Dresselhaus, and T. Koga, Semicond. Semimetals **71**, 1 (2001).
[11] Y. Wu, R. Fan, and P. Yang, Nano Lett. **2**, 83 (2002).
[12] R. S. Wagner and W. C. Ellis, Appl. Phys. Lett. **4**, 89 (1964).
[13] Y. Wu and P. Yang, J. Am. Chem. Soc. **123**, 3165 (2001).
[14] P. Kim, L. Shi, A. Majumdar, and P. L. McEuen, Phys. Rev. Lett. **87**, 215502 (2001).
[15] L. Shi, D. Li, C. Yu, W. Jang, D. Kim, Z. Yao, P. Kim, and A. Majumdar, J. Heat Transfer (in press).
[16] D. Li, Y. Wu, P. Kim, L. Shi, P. Yang, and A. Majumdar, Appl. Phys. Lett. **83**, 2934 (2003).
[17] D. Cahill, W. Ford, K. Goodson, G. Mahan, A. Majumdar, H. Maris, R. Merlin, and S. Phillpot, J. Appl. Phys. **93**, 793 (2003).
[18] D. Cahill, K. Goodson, and A. Majumdar, J. Heat Transfer **124**, 223 (2002).
[19] D. C. Houghton, D. D. Perovic, J.-M. Baribeau, and G. C. Weatherly, J. Appl. Phys. **67**, 1850 (1990).